

# Scaling of diffusion constants in perturbed easy-axis Heisenberg spin chains

Markus Kraft , <sup>\*</sup> Mariel Kempa , Jiaozhi Wang , Sourav Nandy , <sup>2</sup> and Robin Steinigeweg , <sup>†</sup>

<sup>1</sup>University of Osnabrück, Department of Mathematics/Computer Science/Physics, D-49076 Osnabrück, Germany

<sup>2</sup>Max Planck Institute for the Physics of Complex Systems, D-01187 Dresden, Germany

(Dated: August 8, 2025)

Understanding the physics of the integrable spin-1/2 XXZ chain has witnessed substantial progress, due to the development and application of sophisticated analytical and numerical techniques. In particular, infinite-temperature magnetization transport has turned out to range from ballistic, over superdiffusive, to diffusive behavior in different parameter regimes of the anisotropy. Since integrability is rather the exception than the rule, a crucial question is the change of transport under integrability-breaking perturbations. This question includes the stability of superdiffusion at the isotropic point and the change of diffusion constants in the easy-axis regime. In our work, we study this change of diffusion constants by a variety of methods and cover both, linear response theory in the closed system and the Lindblad equation in the open system, where we throughout focus on periodic boundary conditions. In the closed system, we compare results from the recursion method to calculations for finite systems and find evidence for a continuous change of diffusion constants over the full range of perturbation strengths. In the open system weakly coupled to baths, we find diffusion constants in quantitative agreement with the ones in the closed system in a range of nonweak perturbations, but disagreement in the limit of weak perturbations. Using a simple model in this limit, we point out the possibility of a diverging diffusion constant in such an open system.

## I. INTRODUCTION

The study of nonequilibrium processes in quantum many-body systems continues to be one of the central endeavors in different fields of modern physics [1–5], ranging from fundamental questions in statistical mechanics to applied questions in material science. In this context, transport is a paradigmatic example of a nonequilibrium process with relevance to closed and open quantum systems alike. The understanding of nonequilibrium physics in general and transport in particular has seen substantial progress [6], due to experimental advances, fresh theoretical concepts, and the development of sophisticated analytical techniques and numerical methods.

Within the large class of physically relevant quantum many-body models, integrable systems are rare and play a special role. In particular, the spin-1/2 XXZ chain is a prime example of an integrable system and has been scrutinized in numerous studies. Early on, it has become clear that this model can fail to thermalize, which is also reflected in the ballistic flow of energy [7]. Other observables than energy, however, can have a richer dynamical phase diagram, even at high temperatures. Especially the flow of magnetization is ballistic in the easy-plane regime only, where quasilocal conserved charges have an overlap with the current [8–10]. Otherwise, the transport of magnetization has turned out to be superdiffusive at the isotropic point [11–13] and diffusive in the easy-axis regime [14–20].

Since integrable systems are rather the exception than the rule, nonintegrable systems are the generic situation in physics. While these systems are expected to typically

exhibit diffusive transport, the precise value of diffusion constants constitutes a highly nontrivial question and is a challenge for theory [21–28]. An equally nontrivial question is the dynamical behavior in the close vicinity of integrability [29–35]. This question includes the stability of superdiffusion at the isotropic point [36–40], but also the change of diffusion constants in the easy-axis regime [41–43], where this change might be discontinuous. While such a change is in line with breaking microscopic integrability, it is still unexpected from macroscopic phenomenology, where a small perturbation of a normal conductor does not cause a significant change of the transport coefficient.

In our work, we study this change of diffusion constants by a variety of methods and cover both, linear response theory in the closed system and the Lindblad equation in the open system, where we throughout focus on periodic boundary conditions. In the closed system, we compare results from the recursion method [26] to exact results for finite systems and find evidence for a continuous change of diffusion coefficients over the full range of perturbation strengths. In the open system, we find diffusion constants in quantitative agreement with the ones in the closed system for nonweak perturbations, but disagreement for weak perturbations. Using a simple model, we point out that the open-system diffusion constant might diverge in the weak-perturbation limit.

## II. MODEL AND METHODS

In our work, a central model is the spin-1/2 XXZ chain [6],

$$H = J \sum_{r=1}^N (S_r^x S_{r+1}^x + S_r^y S_{r+1}^y + \Delta S_r^z S_{r+1}^z), \quad (1)$$

<sup>\*</sup> [markus.kraft@uos.de](mailto:markus.kraft@uos.de)

<sup>†</sup> [rsteinig@uos.de](mailto:rsteinig@uos.de)

where the  $S_r^j$  ( $j = x, y, z$ ) are spin-1/2 operators at site  $r$ ,  $N$  is the number of sites,  $J > 0$  is the antiferromagnetic exchange coupling constant, and  $\Delta$  is the anisotropy in the  $z$  direction. For all values of  $\Delta$ , the model in Eq. (1) is integrable and the total magnetization  $S^z = \sum_r S_r^z$  is conserved,  $[S^z, H] = 0$ . Throughout our work, we focus on the easy-axis regime  $\Delta > 1$  and choose the specific value  $\Delta = 1.5$ . It is important to note that we employ periodic boundary conditions,  $S_{N+1}^j = S_1^j$ , in the closed system but also in the open system introduced later.

To break the integrability of the model, we consider two different perturbations. First, interactions between next-to-nearest sites,

$$H_{\text{NNN}} = H + \Delta' \sum_{r=1}^N S_r^z S_{r+2}^z, \quad (2)$$

and, second, a staggered magnetic field,

$$H_B = H + B \sum_{r=1}^N (-1)^r S_r^z. \quad (3)$$

Here, the parameters  $\Delta'$  and  $B$  are the corresponding perturbation strengths. For all values of  $\Delta'$  and  $B$ , also including the case  $\Delta' = B = 0$ , transport is expected to be diffusive in the easy-axis regime.

In the closed system, we rely on linear response theory (LRT) [44], where an essential role is played by the operator of the magnetization current [6]

$$j = J \sum_{r=1}^N (S_r^x S_{r+1}^y - S_r^y S_{r+1}^x) \quad (4)$$

and its autocorrelation function

$$\langle j j(t) \rangle = \frac{\text{tr}[e^{-\beta H} e^{i H t} j e^{-i H t} j]}{Z}, \quad Z = \text{tr}[e^{-\beta H}], \quad (5)$$

where  $\beta = 1/T$  is the inverse temperature. In our work, we focus on the high-temperature case  $\beta = 0$ . To study diffusion constants, we define the quantity [45]

$$D(t) = \frac{1}{\chi} \int_0^t dt' \langle j(t') j \rangle, \quad (6)$$

with the static susceptibility  $\chi = 1/4$  for  $\beta = 0$ . In this way, diffusion constants  $D = \lim_{t \rightarrow \infty} \lim_{N \rightarrow \infty} D(t)$  can be obtained, where the order of limits is crucial. In practice, however, one has often access to finite systems only, and then a finite-size scaling is unavoidable. In such a finite-size scaling, the choice of a proper time scale can be a subtle task, as discussed later in detail. Moreover, this finite-size scaling can also depend on the choice of the specific ensemble, and extrapolations can differ for the grandcanonical ensemble  $\langle S^z \rangle = 0$  (all magnetization sectors) and the canonical ensemble  $S^z = 0$  (only zero magnetization sector).

In our work, we apply dynamical quantum typicality for the numerical calculation of the quantity in Eq.

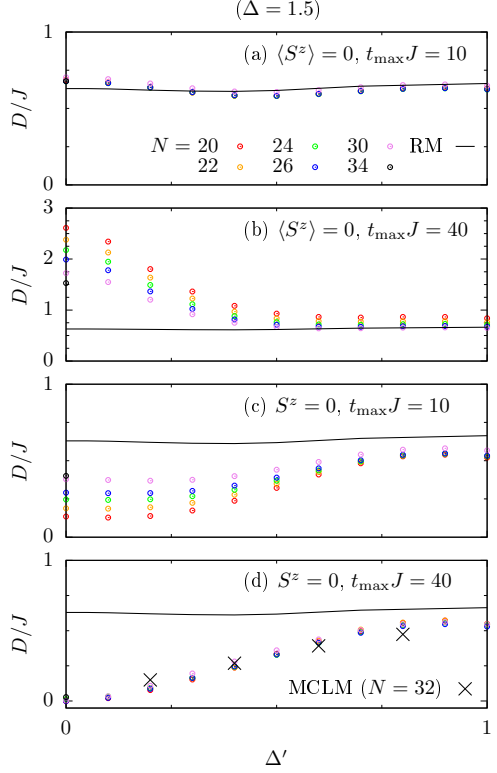


FIG. 1. Diffusion constant  $D$  versus perturbation strength  $\Delta'$  for the model  $H_{\text{NNN}}$  in Eq. (2) with anisotropy  $\Delta = 1.5$ , as calculated numerically by dynamical quantum typicality for different system sizes  $N$  and by the recursion method in the thermodynamic limit [48]. (a)  $\langle S^z \rangle = 0$ ,  $tJ_{\text{max}} = 10$ . (b)  $\langle S^z \rangle = 0$ ,  $tJ_{\text{max}} = 40$ . (c)  $S^z = 0$ ,  $tJ_{\text{max}} = 10$ . (d)  $S^z = 0$ ,  $tJ_{\text{max}} = 40$ . In (d), existing results from the microcanonical Lanczos method are also depicted [42].

(6), which allows us to treat comparatively large system sizes outside the range of standard exact diagonalization [46, 47]. This approach to finite systems is complemented by another technique, which is designed to numerically calculate  $D$  directly in the thermodynamical limit. This technique is a recently proposed recursion method (RM) [26] and is based on Lanczos coefficients in Liouville space. Details of this method can be found in the Appendix A.

In addition to the closed systems discussed so far, we further consider open systems and study nonequilibrium transport, as resulting by the coupling to two baths. To this end, we use the Lindblad equation [49]

$$\dot{\rho}(t) = \mathcal{L}\rho(t) = i[\rho(t), H] + \mathcal{D}\rho(t), \quad (7)$$

where the first term on the r.h.s. describes the unitary time evolution of a density matrix  $\rho(t)$  in the isolated situation, while the second term on the r.h.s. describes nonunitary damping due to the baths and reads

$$\mathcal{D}\rho(t) = \sum_j \alpha_j \left( L_j \rho(t) L_j^\dagger - \frac{1}{2} \{ \rho(t), L_j^\dagger L_j \} \right) \quad (8)$$

with non-negative rates  $\alpha_j$ , Lindblad operators  $L_j$ , and the anticommutator  $\{\bullet, \bullet\}$ . The Lindblad equation is the most general form of a quantum master equation, which is local in time and maps a density matrix to a density matrix again [49]. In the specific context of nonequilibrium transport, a common choice for the Lindblad operators is given by [6]

$$L_1 = S_1^+, L_2 = S_1^-, L_3 = S_{N/2+1}^+, L_4 = S_{N/2+1}^-, \quad (9)$$

which, in our case of periodic boundary conditions, are located at site  $r = 1$  and  $r = N/2 + 1$ . The corresponding rates read  $\alpha_1 = \gamma(1 + \mu)$ ,  $\alpha_2 = \gamma(1 - \mu)$ ,  $\alpha_3 = \gamma(1 - \mu)$ ,  $\alpha_4 = \gamma(1 + \mu)$ , where  $\gamma$  is the system-bath coupling and  $\mu$  is the driving strength. In this setup, a nonequilibrium steady state results in the long-time limit, which features a constant current and a characteristic density profile. In case of normal transport, the diffusion constant is given by the ratio

$$D = -\frac{\langle j_r \rangle}{\langle S_{r+1}^z \rangle - \langle S_r^z \rangle} \quad (10)$$

for some site  $r$  in the bulk. We determine this diffusion constant for small-system bath coupling  $\gamma/J = 0.1$  and weak driving  $\mu = 0.1$ .

A practical advantage of the Lindblad equation is that it can be solved by sophisticated numerical techniques,

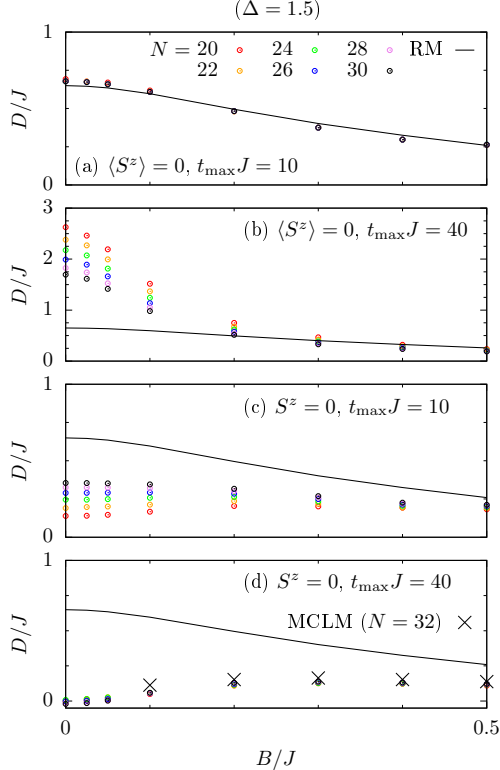


FIG. 2. Similar data as the one in Fig. 1, but now for the model  $H_B$  in Eq. (3).

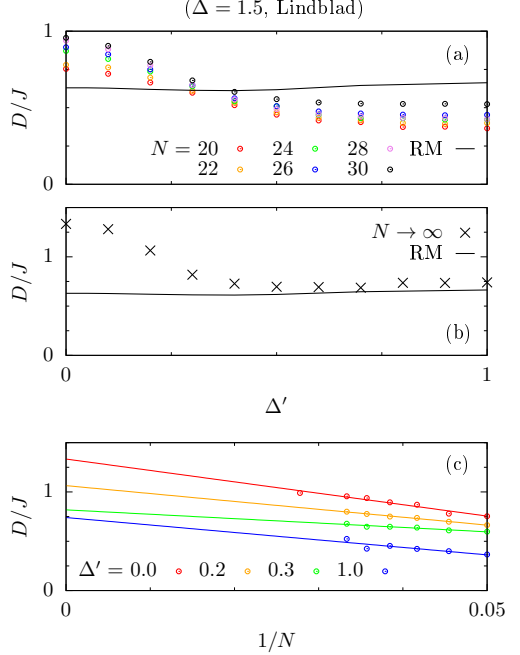


FIG. 3. (a) Diffusion constant  $D$  versus perturbation strength  $\Delta'$  for the model  $H_{\text{NNN}}$  in Eq. (2) with anisotropy  $\Delta = 1.5$ , as calculated numerically in the open system for different system sizes  $N$ . A comparison to the closed-system results from the recursion method is also indicated. (b) Extrapolation to the thermodynamic limit based on the linear scaling in (c).

like stochastic unraveling [15, 50] or simulations based on matrix product states (MPS) [51–53]. In particular, MPS simulations are feasible for quite large system sizes. Yet, they are restricted to open boundary conditions and to large values of the system-bath coupling  $\gamma$ , due to the required reduction of entanglement growth. Thus, we use as an alternative strategy a recently proposed approach [54–56]. On the one hand, this approach is suitable for periodic boundary conditions and small system-bath coupling  $\gamma$  [57]. On the other hand, it allows us to predict the open-system dynamics just on the knowledge of spatio-temporal correlation functions in the closed systems, which in turn enables us to treat open systems outside the range of exact diagonalization and stochastic unraveling. Details on this approach can be found in the Appendix B.

### III. RESULTS

We now move on to our results, starting with the closed-system scenario and the model in Eq. (2). We first focus on results from the recursion method, which are, as discussed in the Appendix A, well converged w.r.t. to the number of Lanczos coefficients and depicted in Fig. 1 (a). As clearly visible, the diffusion constant  $D$  has a continuous dependence on the perturbation strength  $\Delta'$ , with no obvious signature of a discontinuity in the weak-

perturbation limit  $\Delta' \rightarrow 0$ . Furthermore, for the values of  $\Delta'$  considered,  $D(\Delta')$  has a minor dependence on  $\Delta'$  and is an almost flat curve.

In addition, we compare in Fig. 1 (a) the results from the recursion method to finite-size results for the quantity in Eq. (6) from dynamical quantum typicality, for which raw data can be found in the Appendix A. We do so for the grandcanonical ensemble  $\langle S^z \rangle = 0$  and at a time  $tJ = 10$ . Apparently, the finite-size data is in very good agreement with the recursion method and shows no significant dependence on system size. When redoing the comparison for a longer time  $tJ = 40$  in Fig. 1 (b), the agreement becomes worse, due to finite-size effects at nonweak perturbation strengths  $\Delta'$ . Still, when the system size is increased, the finite-size data gets closer and closer to the result from the recursion method, and they might eventually coincide in the thermodynamic limit.

It is instructive to redo the same comparison for the canonical ensemble  $S^z = 0$  as well. As shown in Fig. 1 (c) for a time  $tJ = 10$ , finite-size effects are significantly larger than before, but they seem to be still consistent with the recursion method. Interestingly, for a longer time  $tJ = 40$  in Fig. 1 (d), finite-size effects seem to be smaller. However, this observation has to be taken with special care, in view of the finite-size effects at shorter times.

In Figs. 2 (a)-(d), we repeat the analysis for the other model in Eq. (3). While  $D(B)$  has a stronger dependence on  $B$ , the overall behavior is very similar to the one of  $D(\Delta')$  in Figs. 1 (a)-(d), which indicates that our results do not depend on the specific perturbation.

Next, we turn to the open-system scenario and focus on the model in Eq. (2) again. In Fig. 3 (a), we summarize

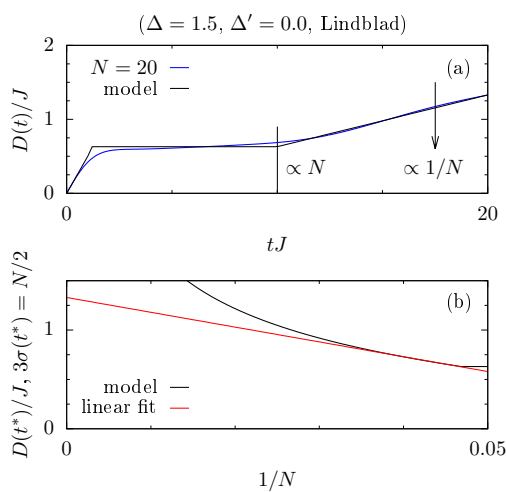


FIG. 4. (a) A simple model for the quantity  $D(t)$  in Eq. (6): After an initial linear increase,  $D(t)$  has a plateau but, after a finite-size time  $\propto N$ , increases linearly with a finite-size slope  $\propto 1/N$ . Free constants are fixed by a fit to  $N = 20$  data for the unperturbed case in Eq. (1). (b) Resulting prediction for the finite-size scaling of the diffusion constant  $D$  in the open systems.

our results for the diffusion constant  $D(\Delta')$ , which we obtain from current and density profile of the steady state in the long-time limit. Apparently,  $D(\Delta')$  differs from the result of the recursion method and increases with system size. To conclude on the thermodynamic limit, we show in Fig. 3 (b) an extrapolation, as resulting from linear fits in Fig. 3 (c). While this extrapolation for  $D(\Delta')$  agrees convincingly with the result of the recursion method in a range of nonweak perturbation strengths  $\Delta'$ , it clearly differs in the limit of weak perturbations  $\Delta' \rightarrow 0$ . This observation suggests that open and closed systems have different diffusion constants in this limit.

#### IV. SIMPLE MODEL

To understand this observation, let us for a moment come back to the closed system and use a simple model for the quantity  $D(t)$  in Eq. (6), as shown in Fig. 4. After an initial linear increase,  $D(t)$  has a plateau but, after a finite-size time  $\propto N$ , increases linearly with a finite-size slope  $\propto 1/N$ . This overall behavior describes well the unperturbed case  $\Delta' = 0$  with periodic boundary conditions [58]. It is worth mentioning that the linear slope is the finite-size Drude weight [6]. Using this model for  $D(t)$ , we can calculate the spreading of an excitation,

$$\sigma^2(t) = 2 \int_0^t dt' D(t'), \quad (11)$$

and determine the time  $t^*$  required to travel through the system,

$$3\sigma(t^*) = \frac{N}{2}. \quad (12)$$

Assuming that  $t^*$  is the relevant time scale for the open system, we plug in  $t^*$  in the original model for  $D(t)$  and use  $D(t^*)$  as a prediction for the diffusion constant in the open system. In Fig. 4 (b), we depict the finite-size scaling of the so obtained  $D(t^*)$ , which is, despite the simplicity of arguments, very similar to the one for the open-system diffusion constant in Fig. 3 (c). Importantly, however,  $D(t^*)$  departs from a  $1/N$ -scaling for large  $N$  and eventually diverges in the limit  $N \rightarrow \infty$ . The departure results from the fact that the steady-state time  $t^*$  increases faster with  $N$  than the time at which  $D(t)$  is converged w.r.t. system size, see Appendix C. This finding opens the possibility of a diverging diffusion constant in the unperturbed open system with periodic boundary conditions. Additional results for open boundary conditions can be found in the Appendix B.

#### V. CONCLUSION

We have analyzed the scaling of diffusion constants under integrability-breaking perturbations of the spin-1/2 XXZ chain in the easy-axis regime. To this end,

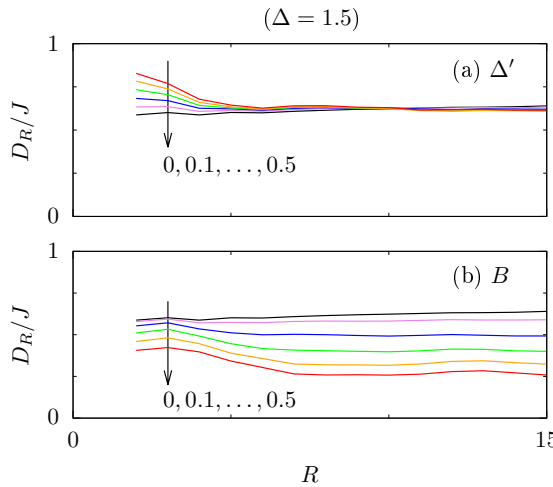


FIG. 5. Diffusion constant  $D_R$  versus  $R$ , as obtained from the recursion method for the model (a)  $H_{\text{NNN}}$  in Eq. (2) and (b)  $H_B$  in Eq. (3).

we have used a variety of methods and covered both, closed and open systems, focusing on periodic boundary conditions. In the closed system, we have found evidence for a continuous change of diffusion constants over the full range of perturbation strengths. In the open system, we have found diffusion constants in quantitative agreement with the ones in the closed system in a range of nonweak perturbations. In the weak-perturbation limit, however, we have found disagreement and also pointed out the possibility of a diverging diffusion constant in the open system.

## ACKNOWLEDGMENTS

We thank Jochen Gemmer, Jacek Herbrych, Zala Lenarčič, Marcin Mierzejewski, and Peter Prelovšek for fruitful discussions.

This work has been funded by the Deutsche Forschungsgemeinschaft (DFG), under Grant No. 531128043, as well as under Grant No. 397107022, No. 397067869, and No. 397082825 within DFG Research Unit FOR 2692, under Grant No. 355031190.

Additionally, we greatly acknowledge computing time on the HPC3 at the University of Osnabrück, granted by the DFG, under Grant No. 456666331. Computations for open boundary conditions were performed at the HPC cluster facility at MPI-PKS Dresden.

## Appendix A: Calculation of equilibrium transport

### 1. Recursion method

Here, we briefly introduce the recursion method, which is used in the main text for the calculation of diffusion

coefficients. It is aiming at a calculation directly in the thermodynamical limit. More details on the method can be found in Ref. [26].

Within this framework, the Laplace transform

$$F(s) = \int_0^\infty dt e^{ts} \tilde{C}(t) \quad (\text{A1})$$

is considered for the autocorrelation function

$$\tilde{C}(t) = \langle \tilde{j}(t) \tilde{j} \rangle, \quad \tilde{j} = \frac{j}{\sqrt{\langle j | j \rangle}} \quad (\text{A2})$$

of the normalized current. In particular,  $\mathcal{F}(0)$  determines the diffusion constant  $D = \langle j^2 \rangle F(0) / \chi$ . According to the Mori formalism, Eq. (A1) can be written in the form

$$F(s) = \frac{1}{s + \frac{b_1^2}{s + \frac{b_2^2}{s + \frac{b_3^2}{s + \dots}}}}, \quad (\text{A3})$$

and one straightforwardly gets

$$D = \frac{\langle j^2 \rangle}{\chi b_1} \prod_{n=1}^{\infty} \left( \frac{b_n}{b_{n+1}} \right)^{(-1)^n}, \quad (\text{A4})$$

where  $b_n$  are the Lanczos coefficients of  $\langle \tilde{j} \rangle$ , the meaning of which will be explained below.

It is now convenient to switch to the Hilbert space of operators and denote its elements  $O$  by states  $|O\rangle$ . This space is equipped with an inner product,

$$\langle O_m | O_n \rangle = \text{tr}[O_m^\dagger O_n], \quad (\text{A5})$$

which defines a norm via

$$\|O\| = \frac{\sqrt{\langle O | O \rangle}}{\text{tr}[1]}. \quad (\text{A6})$$

The Liouvillian (super)operator  $\mathcal{L}$ , which is defined by  $\mathcal{L}|O\rangle = [H, O]$ , propagates a state  $|O\rangle$  in time, such that an autocorrelation function can be written as

$$\langle O(t) O \rangle \propto C(t) = \frac{\langle O | e^{i\mathcal{L}t} | O \rangle}{\|O\|^2}. \quad (\text{A7})$$

We now start the Lanczos iterative scheme, where we choose as the seed operator  $O_0$  the normalized current operator,  $O_0 = \tilde{j}$ . First, we set

$$b_1 = \|\mathcal{L}O_0\|, \quad |O_1\rangle = \frac{\mathcal{L}|O_0\rangle}{b_1}. \quad (\text{A8})$$

Then, we iteratively compute

$$|O'_n\rangle = \mathcal{L}|O_{n-1}\rangle - b_{n-1}|O_{n-2}\rangle \quad (\text{A9})$$

and

$$b_n = \|O'_n\|, \quad |O_n\rangle = \frac{|O'_n\rangle}{b_n}. \quad (\text{A10})$$

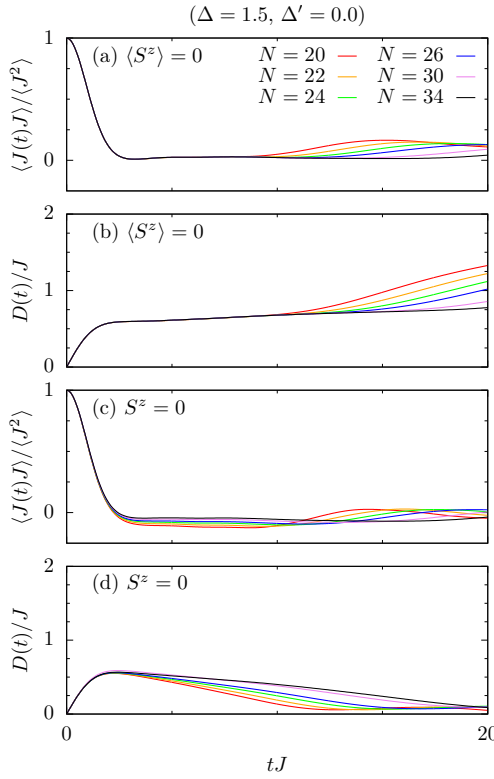


FIG. 6. Decay of the current autocorrelation function  $\langle j(t)j \rangle$  in the unperturbed model in Eq. (1) with anisotropy  $\Delta = 1.5$  for (a) the grandcanonical ensemble  $\langle S^z \rangle = 0$  and (c) the canonical ensemble  $S^z = 0$ , which is numerically calculated for different system sizes  $N$  by the use of dynamical quantum typicality. (b) and (d) Corresponding time dependence of the diffusion coefficients  $D(t)$ .

In this way, all Lanczos coefficients  $b_n$  can in principle be calculated. In practice, however, only the first few  $b_n$  are easily numerically accessible. To this end, we employ the operator growth hypothesis [59], which states that, in a nonintegrable system, the  $b_n$  for sufficiently large  $n$  are asymptotically linear. Assuming [60]

$$b_n = \alpha n + \beta, \quad n \geq R, \quad (\text{A11})$$

one obtains the following approximation of  $F(0)$ :

$$F_0 \approx D_R = \begin{cases} \frac{1}{\tilde{p}_R b_R} \prod_{m=1}^{\frac{R}{2}} \frac{b_{2m}^2}{b_{2m-1}^2} & , \text{ even } R \\ \frac{\tilde{p}_R}{b_R} \prod_{m=1}^{\frac{R-1}{2}} \frac{b_{2m}^2}{b_{2m-1}^2} & , \text{ odd } R \end{cases}, \quad (\text{A12})$$

where

$$p_R = \frac{\Gamma(\frac{R}{2} + \frac{\beta}{2\alpha}) \Gamma(\frac{R}{2} + \frac{\beta}{2\alpha} + 1)}{\Gamma^2(\frac{R}{2} + \frac{\beta}{2\alpha} + \frac{1}{2})}. \quad (\text{A13})$$

Here, we employ a simple approach, where  $\alpha$  and  $\beta$  are determined by  $b_R$  and  $b_{R-1}$  only, i.e.,

$$\alpha_R = b_R - b_{R-1}, \quad \beta_R = Rb_{R-1} - (R-1)b_R. \quad (\text{A14})$$

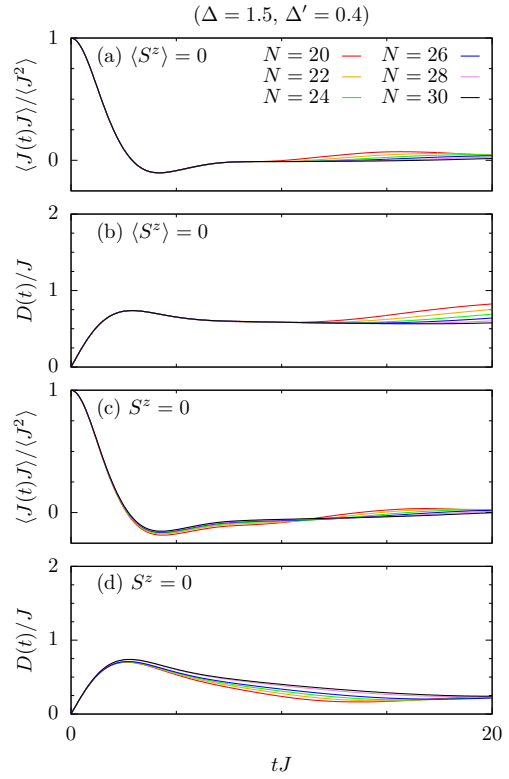


FIG. 7. The same data as in Fig. 6 but now for the model in Eq. (2) with  $\Delta' = 0.4$ .

In Fig. 5, we summarize the so obtained  $D_R$ . As mentioned in the main text,  $D_R$  is well converged w.r.t.  $R$ , for the two models and the perturbation strengths considered.

## 2. Dynamical quantum typicality

Here, we briefly describe our typicality approach to the time dependence of current autocorrelation functions in finite systems. More information on this approach can be found in Refs. [46, 47].

Loosely speaking, the concept of dynamical quantum typicality allows us to replace expectation values w.r.t. ensembles by expectation values w.r.t. single pure states, which are drawn at random from a high-dimensional Hilbert space. In the context of current autocorrelation functions, this concept leads to the approximation

$$\langle j(t)j \rangle = \frac{\langle \psi(t)|j|\varphi(t) \rangle}{\langle \psi(0)|\psi(0) \rangle} + \mathcal{O}\left(\frac{1}{\sqrt{d}}\right), \quad (\text{A15})$$

where  $d = 2^N$  is the dimension of the Hilbert space. The two auxiliary pure states read

$$\psi(t) = e^{-iHt} |\phi\rangle, \quad \varphi(t) = e^{-iHt} j |\phi\rangle, \quad (\text{A16})$$

and  $|\phi\rangle$  is a Haar-random pure state. Importantly, the time argument in the approximation in Eq. (A15) is now

a property of the two pure states and not of the current operator anymore. These pure states can be propagated in time using fourth-order Runge-Kutta or Chebyshev polynomials, which then gives access to comparatively large system sizes outside the range of standard exact diagonalization. An approximation similar to the one in Eq. (A15) can be also obtained for other operators, which we employ for the spatial-temporal correlation functions discussed later in the context of open systems.

In Figs. 6 - 8, we depict raw data for the current autocorrelation function  $\langle j(t)j \rangle$  and its time integral  $D(t)$  for three examples: The integrable model in Eq. (1) and the nonintegrable models in Eqs. (2) [with  $\Delta' = 0.4$ ] and (3) [with  $B/J = 0.3$ ]. We do so for the two ensembles, grandcanonical  $\langle S^z \rangle = 0$  and canonical  $S^z = 0$ . This and similar raw data is the basis of our analysis of diffusion constants in the main text. It is worth mentioning that the finite-size effects are unrelated to the approximation error in Eq. (A15), which is negligibly small in all cases considered.

In Figs. 9 and 10, we additionally depict for the two nonintegrable cases the current autocorrelation function in frequency space, as obtained from a Fourier transform up to a maximum time  $T_{\max}$ . As can be seen, the specific choice of  $T_{\max}$  controls the frequency resolution, and a reasonable choice in a finite system is not obvious. As an additional consistency check of our approach, we compare to existing data from the microcanonical Lanzos method [42] and find a convincing agreement, as visible in Figs. 9 (c) and 10 (d). MCLM data at zero frequency is also shown in the main text.

## Appendix B: Calculation of nonequilibrium transport

### 1. Time evolution of densities

Here, we summarize the main aspects of our approach to the open-system dynamics, which is a prediction just on the basis of the closed-system dynamics. More details on this approach can be found in Refs. [54–56].

Specifically, the prediction is based on spatio-temporal correlation functions at infinite temperature,

$$\langle S_r^z(t)S_{r'}^z(0) \rangle = \frac{\text{tr}[e^{iHt}S_r^z e^{-iHt}S_{r'}^z]}{2^N}. \quad (\text{B1})$$

Before we come to the actual prediction, it is useful to define the quantity

$$C_r(t) = \langle S_r^z(t)S_1^z(0) \rangle - \langle S_r^z(t)S_{N/2+1}^z(0) \rangle, \quad (\text{B2})$$

which is the difference of two correlation functions with  $r' = 1$  and  $r' = N/2+1$ . Further, it is useful to introduce the superposition

$$d_r(t) = 2\mu \sum_j A_j \Theta(t - \tau_j) C_r(t - \tau_j), \quad (\text{B3})$$

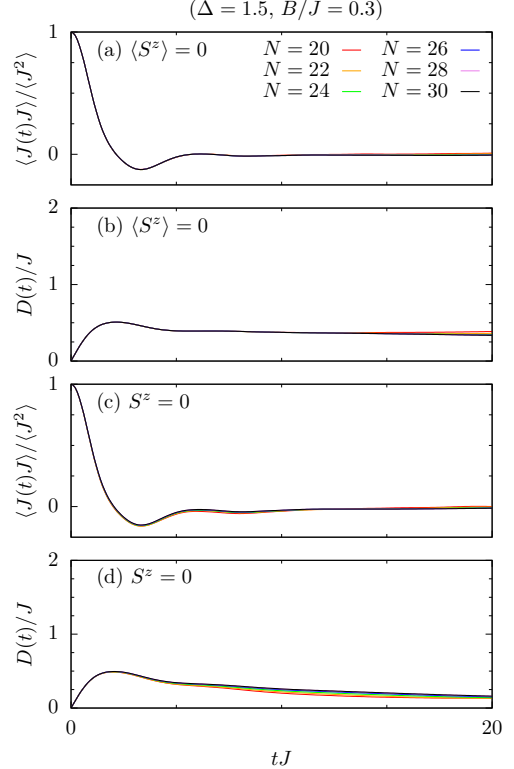


FIG. 8. The same data as in Fig. 6 but now for the model in Eq. (3) with  $B/J = 0.3$ .

where  $A_j$  are some amplitudes,  $\tau_j$  are some times, and  $\Theta(t)$  is the Heavyside function. Using this notation, the prediction for the open-system dynamics can be written as [55]

$$\langle S_r^z(t) \rangle \approx \frac{1}{T_{\max}} \sum_{T=1}^{T_{\max}} d_{r,T}(t), \quad (\text{B4})$$

where the sum runs over  $T_{\max}$  different time sequences  $(\tau_1, \tau_2, \dots)$ . Here, a particular time sequence is generated via

$$\tau_{j+1} = \tau_j - \frac{\ln(\varepsilon_{j+1})}{2\gamma}, \quad (\text{B5})$$

where  $\varepsilon_{j+1}$  are random numbers drawn from a uniform distribution  $[0, 1]$ . The amplitudes  $A_j$  in Eq. (B3) read

$$A_j = \frac{a_j - d_{1,T}(\tau_j - 0^+)}{\mu} \quad (\text{B6})$$

with

$$a_j = \frac{\mu - 2 d_{1,T}(\tau_j - 0^+)}{2 - 4\mu d_{1,T}(\tau_j - 0^+)}. \quad (\text{B7})$$

The accuracy of this prediction has been demonstrated for integrable [55] and nonintegrable [56] systems, and it is particularly high for periodic boundary conditions.

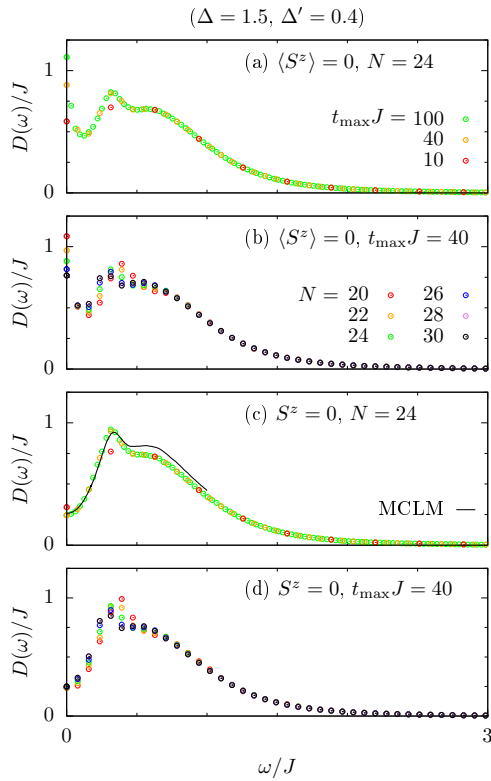


FIG. 9. Diffusion coefficient  $D$  versus frequency  $\omega$  for the model in Eq. (2) with  $\Delta' = 0.4$ , as obtained numerically for the grandcanonical ensemble  $\langle S^z \rangle = 0$  using (a) fixed system size  $N = 24$  and different times  $t_{\max}$  and (b) fixed  $t_{\max}$  and different  $N$ . (c) and (d) show (a) and (b) for the canonical ensemble  $S^z = 0$ . In (c), the MCLM result from Ref. [42] is also depicted.

## 2. Current in the steady state

To obtain the current in the steady state, we need the injected magnetization  $\langle \delta S_1^z \rangle$  at the first bath site, which can be predicted as [55]

$$\langle \delta S_1^z(t) \rangle \approx \frac{1}{T_{\max}} \sum_{T=1}^{T_{\max}} \delta d_{1,T}(t) \quad (B8)$$

with

$$\delta d_{1,T}(t) = 2\mu \sum_j A_j \Theta(t - \tau_j) \langle [S_1^z(0)]^2 \rangle. \quad (B9)$$

In the steady state, all local currents are the same,

$$\langle j_r \rangle = \langle j_{r'} \rangle, \quad 1 \leq r, r' \leq N/2 + 1. \quad (B10)$$

Thus, it is sufficient to know  $\langle j_1 \rangle$  to get all other local currents. In particular,  $\langle j_1 \rangle$  can be obtained from the injected magnetization via [55]

$$\langle j_1 \rangle = \frac{d}{dt} \frac{\langle \delta S_1^z(t) \rangle}{2}, \quad (B11)$$

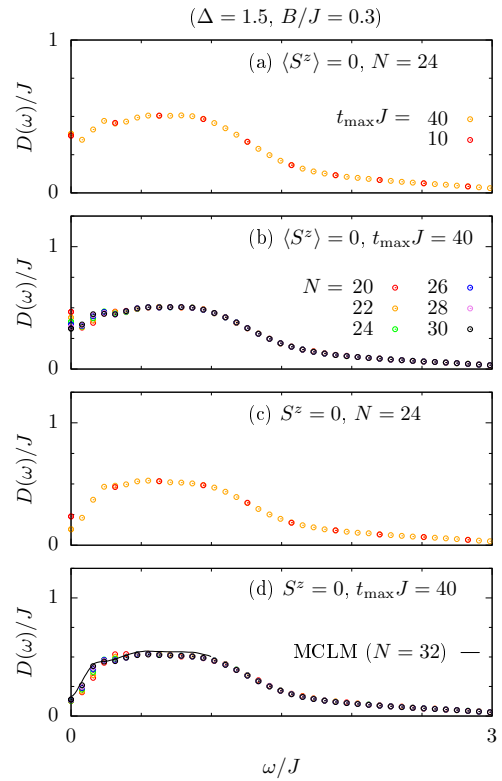


FIG. 10. The same data as in Fig. 9 but now for the model in Eq. (3) with  $B/J = 0.3$ .

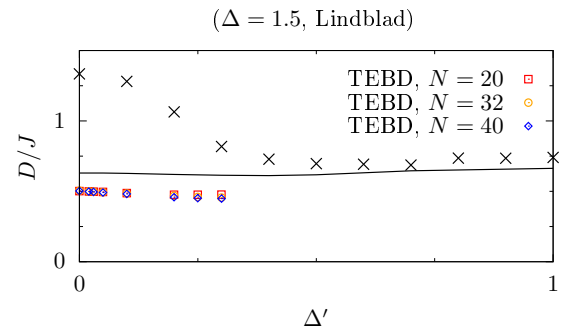


FIG. 11. Open boundary conditions and large system-bath coupling. TEBD data is compared to the results in Fig. 3 (b) of the main text.

where the factor  $1/2$  takes into account that the injected magnetization can flow to the left and to the right of this bath, due to periodic boundary conditions. Then, we can compute the diffusion constant in the steady state by

$$D = -\frac{\langle j_1 \rangle}{\langle S_{r+1}^z \rangle - \langle S_r^z \rangle}, \quad (B12)$$

for some  $r$  in the bulk of the system.

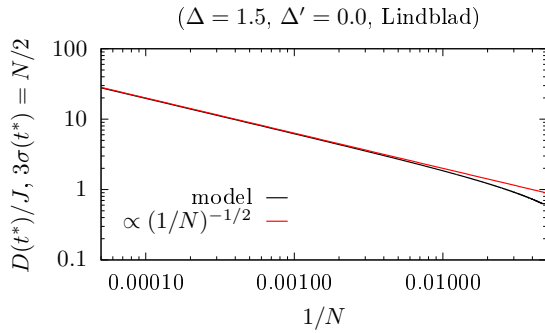


FIG. 12. The same data as in Fig. 4, but now depicted in a log-log plot and compared to the power law  $\propto (1/N)^{-1/2}$ .

### 3. Open boundary conditions

While we have focused throughout the main text on the case of periodic boundary conditions, it is certainly an interesting and important question whether and to what degree the results change for the case of open boundary conditions. Unfortunately, our approach to open systems is less reliable in this case. Instead, we show in Fig. 11 results from time-evolving block decimation (TEBD) for a large system-bath coupling  $\gamma/J = 1$  and compare to the results in Fig. 3 (b) of the main text.

Consistent with the simple model, the TEBD data do not show an increased value of  $D(\Delta')$  for small  $\Delta'$ , as there is no finite-size Drude weight for open boundary conditions. Notably,  $D(\Delta')$  at fixed  $\Delta$  decreases, as the system size  $N$  is increased, at least for the system sizes depicted. While it is hard to conclude on the behavior in the thermodynamic limit, the comparison indicates a sensitivity on the specific boundary conditions employed, which might be traced back to an anomalous character of the integrable point.

## Appendix C: Details on the simple model

### 1. Time-dependent diffusion coefficient

In the main text, we have briefly introduced a simple model for the system-size scaling of the diffusion constant in the open system. Thus, we provide here an extended discussion and further details.

The simple model is based on the closed system and makes an assumption on the time-dependent diffusion coefficient in Eq. (6),

$$D(t) = \frac{1}{\chi} \int_0^t dt' \langle j(t') j \rangle. \quad (\text{C1})$$

Specifically, this assumption reads

$$D(t) = at \Theta(t_1 - t) + b \Theta(t - t_1) + c(t - t_2) \Theta(t - t_2), \quad (\text{C2})$$

where  $\Theta(t)$  is the Heavyside function. Hence,  $D(t)$  first increases linearly up to a time  $t_1$ , then remains constant up to a time  $t_2$ , and finally increases linearly again. In particular, as illustrated in Fig. 4, the quantities  $t_2$  and  $c$  are assumed to depend on system size as [58]

$$t_2 \propto N, \quad c \propto \frac{1}{N}, \quad (\text{C3})$$

while the other quantities  $t_1$ ,  $a$ , and  $b$  are independent of system size. The parameter  $a$  is given by

$$a = \frac{\langle j^2 \rangle}{\chi} = \frac{1}{2} \quad (\text{C4})$$

and the remaining parameters are obtained from a fit to  $N = 20$  data for  $\Delta = 1.5$ ,

$$t_1 = 1.2, \quad t_2 = 0.5 L, \quad b = 0.63, \quad c = \frac{1.4}{N}. \quad (\text{C5})$$

Note that the parameter  $c$  results from a saturation of the current autocorrelation at long times,

$$\lim_{t \rightarrow \infty} \frac{\langle j(t) j \rangle}{\chi} \propto \frac{1}{N}, \quad (\text{C6})$$

and plays the role of the finite-size Drude weight, which is expected to vanish for  $\Delta = 1.5$  and  $N \rightarrow \infty$  [6]. Thus, for  $N \rightarrow \infty$ , the assumption in Eq. (C2) leads to

$$\lim_{t \rightarrow \infty} D(t) = b = \text{const.}, \quad (\text{C7})$$

which indicates normal diffusion, as expected for  $\Delta = 1.5$  [6]. It is worth pointing out that the finite-size Drude weight could in principle hide anomalous behavior,

$$\frac{\langle j(t) j \rangle}{\chi} \propto \frac{1}{t}, \quad (\text{C8})$$

and therefore a logarithmic divergence of the diffusion coefficient,

$$D(t) \propto \log t. \quad (\text{C9})$$

However, numerical simulations like ours in Fig. 6 do not support such an anomalous contribution and already indicate a constant plateau. Moreover, for the following discussion, a potentially anomalous contribution plays a minor role. In fact, the finite-size Drude weight is much more important.

### 2. Real-time broadening

Next, let us stay in the closed system and consider the spatio-temporal correlation functions  $\langle S_r^z(t) S_{r'}^z(0) \rangle$  in Eq. (B1). At  $t = 0$ ,

$$\langle S_r^z(0) S_{r'}^z(0) \rangle = \frac{1}{4} \delta_{r,r'} \quad (\text{C10})$$

at infinite temperature, where  $\delta_{r,r'}$  denotes the Kronecker symbol. Therefore, the profile is initially a sharp peak at the lattice site  $r = r'$ . The real-time broadening of this peak can be followed via the spatial variance,

$$\begin{aligned} \sigma^2(t) &= \sum_r (r - r')^2 \frac{\langle S_r^z(t) S_{r'}^z(0) \rangle}{1/4} \\ &+ \left[ \sum_r (r - r') \frac{\langle S_r^z(t) S_{r'}^z(0) \rangle}{1/4} \right]^2, \end{aligned} \quad (\text{C11})$$

which can be written in the form of Eq. (11),

$$\sigma^2(t) = 2 \int_0^t dt' D(t'), \quad (\text{C12})$$

and is expressed in terms of the time-dependent diffusion coefficient  $D(t)$  in Eq. (6). Note that this expression does not require the assumption for  $D(t)$  in Eq. (C2). Now, let us consider the time  $t^*$ , when the initially sharp peak has broadened over half of the system,

$$3\sigma(t^*) = \frac{N}{2}, \quad (\text{C13})$$

where we take three times the standard deviation for sake of simplicity. Using the assumption in Eq. (C2),  $t^*$  can then be calculated for any system size  $N$ . For large  $N$ , one finds the asymptotic behavior

$$t^* \propto N^{3/2} \quad (\text{C14})$$

and, in particular,  $t^* \gg t_2$ . For normal diffusion, as a side remark, one would have  $t^* \propto N^2$ .

### 3. Link to the open system

Eventually, let us link to the actual open system. To this end, we assume that, for the open system, (i)  $t^*$  is the relevant time scale and that (ii)  $D(t = t^*)$ , evaluated at  $t = t^*$ , is the corresponding diffusion coefficient. Note that these two assumptions are reasonable, in view of the correspondence between closed and open systems in and around Eq. (B4).

In Fig. 4, we have shown the finite-size scaling of the so obtained  $D(t^*)$ . On the one hand,  $D(t^*)$  agrees nicely with the  $1/N$  scaling, as suggested by numerics for small system sizes, which serves as a consistency check. On the other hand,  $D(t^*)$  departs from a  $1/N$  scaling for larger system sizes. To conclude on the asymptotic behavior, we show in Fig. 12 the same data as in Fig. 4, but now depicted in a log-log plot. Clearly,

$$D(t^*) \propto \sqrt{N}, \quad (\text{C15})$$

which can be also seen easily by plugging the asymptotic behavior of the time  $t^* \propto N^{3/2}$  into the assumption for the diffusion coefficient in Eq. (C2).

We should stress that the assumption in Eq. (C2) is only applicable to the integrable point. For the case of a weak but nonvanishing perturbation, this assumption is only expected to hold up to a certain system size. Above this system size, the scaling of the Drude weight changes from a power law to an exponential decrease in system size, which is consistent with the eigenstate thermalization hypothesis [61] and in turn leads to a convergence of the diffusion coefficient w.r.t. system size.

---

[1] I. Bloch, J. Dalibard, and W. Zwerger, *Many-body physics with ultracold gases*, *Rev. Mod. Phys.* **80**, 885 (2008).

[2] A. Polkovnikov, K. Sengupta, A. Silva, and M. Vengalattore, *Colloquium: Nonequilibrium dynamics of closed interacting quantum systems*, *Rev. Mod. Phys.* **83**, 863 (2011).

[3] J. Eisert, M. Friesdorf, and C. Gogolin, *Quantum many-body systems out of equilibrium*, *Nat. Phys.* **11**, 124 (2015).

[4] L. D'Alessio, Y. Kafri, A. Polkovnikov, and M. Rigol, *From quantum chaos and eigenstate thermalization to statistical mechanics and thermodynamics*, *Adv. Phys.* **65**, 239 (2016).

[5] D. A. Abanin, E. Altman, I. Bloch, and M. Serbyn, *Colloquium: Many-body localization, thermalization, and entanglement*, *Rev. Mod. Phys.* **91**, 021001 (2019).

[6] B. Bertini, F. Heidrich-Meisner, C. Karrasch, T. Prosen, R. Steinigeweg, and M. Žnidarič, *Finite-temperature transport in one-dimensional quantum lattice models*, *Rev. Mod. Phys.* **93**, 025003 (2021).

[7] X. Zotos, F. Naef, and P. Prelovsek, *Transport and conservation laws*, *Phys. Rev. B* **55**, 11029 (1997).

[8] T. Prosen, *Open XXZ spin chain: Nonequilibrium steady state and a strict bound on ballistic transport*, *Phys. Rev. Lett.* **106**, 217206 (2011).

[9] T. Prosen and E. Ilievski, *Families of quasilocal conservation laws and quantum spin transport*, *Phys. Rev. Lett.* **111**, 057203 (2013).

[10] E. Ilievski, M. Medenjak, T. Prosen, and L. Zadnik, *Quasilocal charges in integrable lattice systems*, *J. Stat. Mech.: Theory Exp.* **2016**, 064008 (2016).

[11] M. Žnidarič, *Spin transport in a one-dimensional anisotropic Heisenberg model*, *Phys. Rev. Lett.* **106**, 220601 (2011).

[12] E. Ilievski, J. De Nardis, M. Medenjak, and T. Prosen, *Superdiffusion in one-dimensional quantum lattice models*, *Phys. Rev. Lett.* **121**, 230602 (2018).

[13] M. Ljubotina, M. Žnidarič, and T. Prosen, *Kardar-Parisi-Zhang physics in the quantum Heisenberg magnet*, *Phys. Rev. Lett.* **122**, 210602 (2019).

[14] P. Prelovsek, S. E. Shawish, X. Zotos, and M. Long, *Anomalous scaling of conductivity in integrable fermion systems*, *Phys. Rev. B* **70**, 205129 (2004).

[15] M. Michel, O. Hess, H. Wichterich, and J. Gemmer, *Transport in open spin chains: A Monte Carlo wavefunction approach*, *Phys. Rev. B* **77**, 104303 (2008).

[16] T. Prosen and M. Žnidarič, *Matrix product simulations*

of non-equilibrium steady states of quantum spin chains, *J. Stat. Mech.* **2009**, P02035 (2009).

[17] R. Steinigeweg and W. Brenig, *Spin transport in the XXZ chain at finite temperature and momentum*, *Phys. Rev. Lett.* **107**, 250602 (2011).

[18] C. Karrasch, J. E. Moore, and F. Heidrich-Meisner, *Real-time and real-space spin and energy dynamics in one-dimensional spin-1/2 systems induced by local quantum quenches at finite temperatures*, *Phys. Rev. B* **89**, 075139 (2014).

[19] J. De Nardis, D. Bernard, and B. Doyon, *Diffusion in generalized hydrodynamics and quasiparticle scattering*, *SciPost Phys.* **6**, 049 (2019).

[20] S. Gopalakrishnan and R. Vasseur, *Kinetic theory of spin diffusion and superdiffusion in XXZ spin chains*, *Phys. Rev. Lett.* **122**, 127202 (2019).

[21] R. Steinigeweg, F. Heidrich-Meisner, J. Gemmer, K. Michielsen, and H. De Raedt, *Scaling of diffusion constants in the spin-1/2 XX ladder*, *Phys. Rev. B* **90**, 094417 (2014).

[22] B. Kloss, Y. B. Lev, and D. Reichman, *Time-dependent variational principle in matrix-product state manifolds: Pitfalls and potential*, *Phys. Rev. B* **97**, 024307 (2018).

[23] J. Richter and R. Steinigeweg, *Combining dynamical quantum typicality and numerical linked cluster expansions*, *Phys. Rev. B* **99**, 094419 (2019).

[24] J. Wurtz and A. Polkovnikov, *Quantum diffusion in spin chains with phase space methods*, *Phys. Rev. E* **101**, 052120 (2020).

[25] T. Rakovszky, C. W. von Keyserlingk, and F. Pollmann, *Dissipation-assisted operator evolution method for capturing hydrodynamic transport*, *Phys. Rev. B* **105**, 075131 (2022).

[26] J. Wang, M. H. Lamann, R. Steinigeweg, and J. Gemmer, *Diffusion constants from the recursion method*, *Phys. Rev. B* **110**, 104413 (2024).

[27] S. Yi-Thomas, B. Ware, J. D. Sau, and C. D. White, *Comparing numerical methods for hydrodynamics in a one-dimensional lattice spin model*, *Phys. Rev. B* **110**, 134308 (2024).

[28] C. Artiaco, C. Fleckenstein, D. Aceituno Chávez, T. K. Kvorning, and J. H. Bardarson, *Efficient large-scale many-body quantum dynamics via local-information time evolution*, *PRX Quantum* **5**, 020352 (2024).

[29] P. Jung, R. W. Helmes, and A. Rosch, *Transport in almost integrable models: Perturbed Heisenberg chains*, *Phys. Rev. Lett.* **96**, 067202 (2006).

[30] P. Jung and A. Rosch, *Spin conductivity in almost integrable spin chains*, *Phys. Rev. B* **76**, 245108 (2007).

[31] R. Steinigeweg, J. Herbrych, X. Zotos, and W. Brenig, *Heat conductivity of the Heisenberg spin-1/2 ladder: From weak to strong breaking of integrability*, *Phys. Rev. Lett.* **116**, 017202 (2016).

[32] M. Brenes, E. Mascarenhas, M. Rigol, and J. Goold, *High-temperature coherent transport in the XXZ chain in the presence of an impurity*, *Phys. Rev. B* **98**, 235128 (2018).

[33] M. Žnidarič, *Weak integrability breaking: Chaos with integrability signature in coherent diffusion*, *Phys. Rev. Lett.* **125**, 180605 (2020).

[34] A. Bastianello, A. D. Luca, and R. Vasseur, *Hydrodynamics of weak integrability breaking*, *J. Stat. Mech.: Theory Exp.* **2021**, 114003 (2021).

[35] M. Žnidarič, *Modified Matthiessen's rule: More scattering leads to less resistance*, *Phys. Rev. B* **105**, 045140 (2022).

[36] J. De Nardis, S. Gopalakrishnan, R. Vasseur, and B. Ware, *Stability of superdiffusion in nearly integrable spin chains*, *Phys. Rev. Lett.* **127**, 057201 (2021).

[37] D. Roy, A. Dhar, H. Spohn, and M. Kulkarni, *Robustness of Kardar-Parisi-Zhang scaling in a classical integrable spin chain with broken integrability*, *Phys. Rev. B* **107**, L100413 (2023).

[38] S. Nandy, Z. Lenarčič, E. Ilievski, M. Mierzejewski, J. Herbrych, and P. Prelovšek, *Spin diffusion in a perturbed isotropic Heisenberg spin chain*, *Phys. Rev. B* **108**, L081115 (2023).

[39] S. Gopalakrishnan and R. Vasseur, *Superdiffusion from nonabelian symmetries in nearly integrable systems*, *Annu. Rev. Condens. Matter Phys.* **15**, 159 (2024).

[40] A. J. McRoberts and R. Moessner, *Parametrically long lifetime of superdiffusion in non-integrable spin chains*, *arXiv:2402.18662* (2024).

[41] J. De Nardis, S. Gopalakrishnan, R. Vasseur, and B. Ware, *Subdiffusive hydrodynamics of nearly integrable anisotropic spin chains*, *Proc. Natl. Acad. Sci. USA* **119** (2022).

[42] P. Prelovšek, S. Nandy, Z. Lenarčič, M. Mierzejewski, and J. Herbrych, *From dissipationless to normal diffusion in the easy-axis Heisenberg spin chain*, *Phys. Rev. B* **106**, 245104 (2022).

[43] J. Pawłowski, M. Mierzejewski, and P. Prelovsek, *Transport in integrable and perturbed easy-axis heisenberg chain: Thouless approach*, *arXiv:2501.03735* (2025).

[44] R. Kubo, M. Toda, and N. Hashisume, *Statistical physics II: Nonequilibrium statistical mechanics*, Springer Series in Solid-State Sciences Vol. 31 (Springer, Berlin, 1991).

[45] R. Steinigeweg, H. Wichterich, and J. Gemmer, *Density dynamics from current auto-correlations at finite time- and length-scales*, *EPL (Europhys. Lett.)* **88**, 10004 (2009).

[46] T. Heitmann, J. Richter, D. Schubert, and R. Steinigeweg, *Selected applications of typicality to real-time dynamics of quantum many-body systems*, *Z. Naturforsch. A* **75**, 421 (2020).

[47] F. Jin, D. Willsch, M. Willsch, H. Lagemann, K. Michielsen, and H. De Raedt, *Random state technology*, *J. Phys. Soc. Jpn.* **90**, 012001 (2021).

[48] Even though the results from the recursion method are indicated by a solid line in Fig. 1, these results are also obtained for a discrete set of perturbation strengths (see Appendix A).

[49] H.-P. Breuer and F. Petruccione, *The theory of open quantum systems* (Oxford University Press, 2007).

[50] J. Dalibard, Y. Castin, and K. Mølmer, *Wave-function approach to dissipative processes in quantum optics*, *Phys. Rev. Lett.* **68**, 580 (1992).

[51] G. Vidal, *Efficient classical simulation of slightly entangled quantum computations*, *Phys. Rev. Lett.* **91**, 147902 (2003).

[52] G. Vidal, *Efficient simulation of one-dimensional quantum many-body systems*, *Phys. Rev. Lett.* **93**, 040502 (2004).

[53] F. Verstraete, V. Murg, and J. I. Cirac, *Matrix product states, projected entangled pair states, and variational renormalization group methods for quantum spin systems*, *Adv. Phys.* **57**, 143 (2008).

[54] T. Heitmann, J. Richter, J. Herbrych, J. Gemmer, and R. Steinigeweg, *Real-time broadening of bath-induced*

*density profiles from closed-system correlation functions*, *Phys. Rev. E* **108**, 024102 (2023).

[55] T. Heitmann, J. Richter, F. Jin, S. Nandy, Z. Lenarčič, J. Herbrych, K. Michielsen, H. De Raedt, J. Gemmer, and R. Steinigeweg, *Spin-1/2 XXZ chain coupled to two Lindblad baths: Constructing nonequilibrium steady states from equilibrium correlation functions*, *Phys. Rev. B* **108**, L201119 (2023).

[56] M. Kraft, J. Richter, F. Jin, S. Nandy, J. Herbrych, K. Michielsen, H. De Raedt, J. Gemmer, and R. Steinigeweg, *Lindblad dynamics from spatio-temporal correlation functions in nonintegrable spin-1/2 chains with different boundary conditions*, *Phys. Rev. Res.* **6**, 023251 (2024).

[57] The choice of  $\gamma$  can potentially influence the value of the diffusion constant [62].

[58] R. Steinigeweg, J. Herbrych, P. Prelovšek, and M. Mierzejewski, *Coexistence of anomalous and normal diffusion in integrable Mott insulators*, *Phys. Rev. B* **85**, 214409 (2012).

[59] D. E. Parker, X. Cao, A. Avdoshkin, T. Scaffidi, and E. Altman, *A universal operator growth hypothesis*, *Phys. Rev. X* **9**, 041017 (2019).

[60] While the linear scaling in Eq. (A11) is only expected to hold in nonintegrable systems, we also use it for the integrable point. As discussed in [26], the specific form of the scaling function is less important than the required absence of fluctuations.

[61] R. Steinigeweg, J. Herbrych, and P. Prelovšek, *Eigenstate thermalization within isolated spin-chain systems*, *Phys. Rev. E* **87**, 012118 (2013).

[62] R. Steinigeweg, M. Ogiewa, and J. Gemmer, *Equivalence of transport coefficients in bath-induced and dynamical scenarios*, *EPL (Europhys. Lett.)* **87**, 10002 (2009).